Chemical Science

Accepted Manuscript

This article can be cited before page numbers have been issued, to do this please use: R. J. Ortiz, D. Nemez, M. Bhuiyan, K. A. Veilleux and D. E. Herbert, *Chem. Sci.*, 2026, DOI: 10.1039/D6SC01462C.

ROYAL SOCIETY OF CHEMISTRY

rsc.li/chemical-science

View Article Online
DOI: 10.1039/D6SC01462C

COMMUNICATION

Received 00th January 20xx,
Accepted 00th January 20xx

DOI: 10.1039/x0xx00000x

Deep Red Photocatalysis via Direct $S_0 \rightarrow T_1$ Excitation of an Ir(III) Complex using 740 nm Light

Robert J. Ortiz,[a] Dion B. Nemez,[a] Mahtasim Bhuiyan,[a] Keighlynn A. Veilleux,[a] David E. Herbert*[a]

Abstract We report the first examples of deep-red Ir(III) photochemistry using $[Ir(ppy)_2(p\text{-biphe})]PF_6$ (ppy = 2-phenylpyridine; p-biphe = 6,6',7,7'-biphenanthridine). Red light (740 nm) directly excites into the triplet manifold, populating a long-lived excited state (54 ± 3 ns) with mixed triplet metal-to-ligand charge-transfer / ligand-centered character capable of energy-transfer and electron-transfer photocatalysis.

While photocatalysis is by now an established pillar of modern synthetic chemistry,[1] the majority of reactions utilize higher energy visible light (~390-550 nm).[2] Longer wavelengths, notably red (600-700 nm) and near infrared (NIR) light, can penetrate deeper into solutions compared with shorter wavelengths, decreasing the chance of side reactions involving direct absorption by substrates/products, and lowering the probability of catalyst degradation, alongside the safety benefits of utilizing lower energy radiation.[3] In addition to metalloporphyrins and related molecules, and emerging work with abundant-element chromophores,[4] coordination complexes of osmium(II) and ruthenium(II) have arguably received the most attention in this area (**Figure 1**).[5] In these latter cases, the photophysics exploits the ability of heavier elements to undergo direct, spin-forbidden $S_0 \rightarrow T_1$ excitation thanks to large spin-orbit coupling (SOC).[6] Despite this success with heavier Group 8 elements[7] and the general utility of Ir(III) photocatalysis,[8] red-light mediated processes using Group 9 chromophores has remained elusive.[9,10] The lowest energy excitation reached with photochemically active Ir(III) has been orange light (590 nm).[10] This presents an opportunity for ligand design to access deeper red excitation with Ir(III).

We recently reported the synthesis of $[Ir(ppy)_2(p\text{-biphe})]PF_6$ ($[\mathbf{Ir}]PF_6$) a heteroleptic Ir(III) complex supported by 2-phenylpyridine (ppy) and a 6,6',7,7'-biphenanthridine ligand (p-biphe).[11] The planar, π-extended p-biphe framework[12] allows $[\mathbf{Ir}]^+$ to absorb throughout the visible region of the electromagnetic spectrum past 800 nm, and emit in the NIR. The broad absorption intrigued us with respect to the possibility of leveraging low-energy light in photocatalysis.

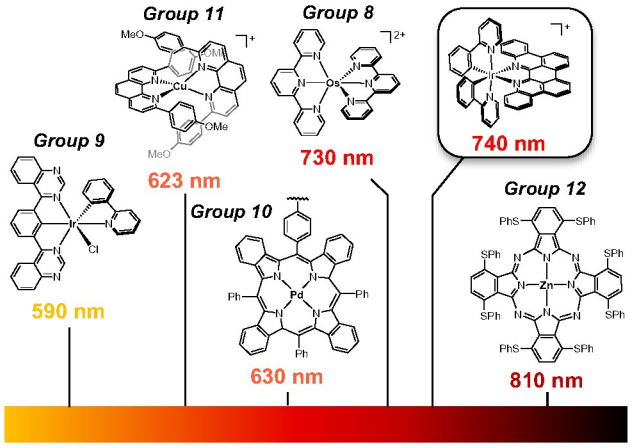

Figure 1. Low-energy photocatalysts in literature[4,5] and the $[Ir(ppy)_2(p\text{-biphe})]^+$ complex ($[\mathbf{Ir}]^+$) that is the focus of this work.

In particular, a weak band (ε ~ 220 M^{-1} cm^{-1}) is evident in the absorption spectrum of $[\mathbf{Ir}]^+$, assigned to direct $S_0 \rightarrow T_n$ transitions. Exploiting this absorption using 740 nm red LEDs would represent a 150 nm (3400 cm^{-1}) bathochromic shift compared to state-of-the-art low-energy Ir photocatalysts.[9,10] The UV-Vis spectrum of a concentrated sample of $[\mathbf{Ir}]PF_6$ (0.8 mM) clearly resolves three peaks in the lowest energy region (**Figure 2a**) which can be fit by Gaussian deconvolution (**Figure S1**).[13] Density functional theory (DFT) and time-dependent DFT simulations including SOC assigns these as spin-forbidden $S_0 \rightarrow T_1$ (783 nm) and $S_0 \rightarrow T_2$ (717 nm) transitions, overlapping with the spin-allowed $S_0 \rightarrow S_1$ (605 nm; **Figure S2** and **Table S1**). Electron-hole density maps indicate the lowest energy $S_0 \rightarrow T_1$ band has mixed metal-to-ligand charge-transfer / ligand centered (^{3}MLCT/^{3}LC) character, while the higher energy $S_0 \rightarrow T_2$

[a] Department of Chemistry and the Manitoba Institute for Materials, University of Manitoba, 144 Dysart Road, Winnipeg, MB, R3T 2N2, Canada; *david.herbert@umanitoba.ca

View Article Online
DOI: 10.1039/D6SC01462C

and $S_0 \rightarrow S_1$ bands present MLCT/inter-ligand charge-transfer (MLCT/ILCT) character. These bands should be directly accessible using red LEDs (red spectrum in **Figure 2a**).

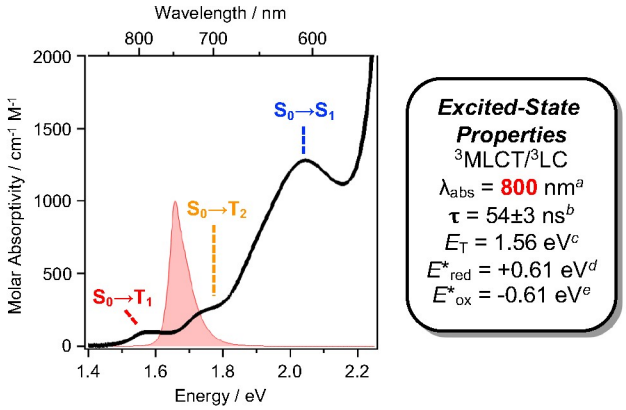

Figure 2. (a) The low-energy absorption spectrum of [**Ir**]PF_6 with assigned transitions based on computational analysis, overlaid with the emission profile of the red LED light source used for photocatalysis. (b) Excited state properties: [a] $S_0 \rightarrow T_1$ transition; [b] from oTA spectroscopy; [c] from highest energy vibrational band in the emission spectrum at 77 K; [d] $E_{red}^* = E_{red} + E_T$; [e] $E_{ox}^* = E_{ox} - E_T$, vs $FcH^{0/+}$

Phosphorescence from [**Ir**]PF_6 (λ_{em} = 812 nm; Φ_{lum} = 0.26%), is sufficiently bright to record the lifetime of the emissive state (τ = 55 ns).[11] Optical transient absorption (oTA) spectroscopy measurements of [**Ir**]PF_6 in acetonitrile using a 540 nm pump confirms formation of a single, dominant excited state. The spectrum taken at a 13 ns delay shows excited-state absorptions (ESA) between 350-470 nm and 540-700 nm sandwiching a shallow bleach (480-530 nm; **Figure 3a**). A linear combination of the absorption spectra of oxidized/reduced [**Ir**]PF_6 measured in a spectroelectrochemical cell (**Figures S3-S4**) shows good but not perfect agreement with these features, supporting an interconfigurational ^{3}LC/^{3}MLCT assignment with characteristics of the MLCT state (**Figure 3b**). Single-wavelength kinetic traces monitored at 600 nm can be fit to a single-exponential decay with a time constant of 54 ± 3 ns (**Figure 3c**), in excellent agreement with the time constant extracted from luminescence decay measurements in dichloromethane.[11] Overall, the 54 ns lifetime measured for the excited state of [**Ir**]$^+$ should be more than sufficient for bimolecular quenching.

Cyclic voltammetry (CV) shows [**Ir**]$^+$ can be reversibly reduced at -0.95 V and -1.53 V vs. $FcH^{0/+}$ (FcH = ferrocene), with an irreversible oxidation at +0.95 V.[11] The triplet state energy can be calculated at 1.56 eV using the highest energy emission band recorded at 77 K (**Figure S5**).[14] Using these data, we estimate excited-state redox potentials of E_{red}^* = +0.61 V, and E_{ox}^* = -0.61 V vs $FcH^{0/+}$.[15] [**Ir**]$^+$ thus could conceivably serve both as a strong photo-oxidant and photo-reductant.[16] Given the irreversible nature of the oxidation event recorded by CV, we chose to target reactions in which the substrate is oxidized, as well as energy-transfer photocatalysis. This choice was bolstered by the observation that known low-energy Ir(III) photocatalysts are generally reducing,[10] differentiating the photochemical reactivity possible with [**Ir**]PF_6. Important excited-state parameters are summarized in **Figure 2**.

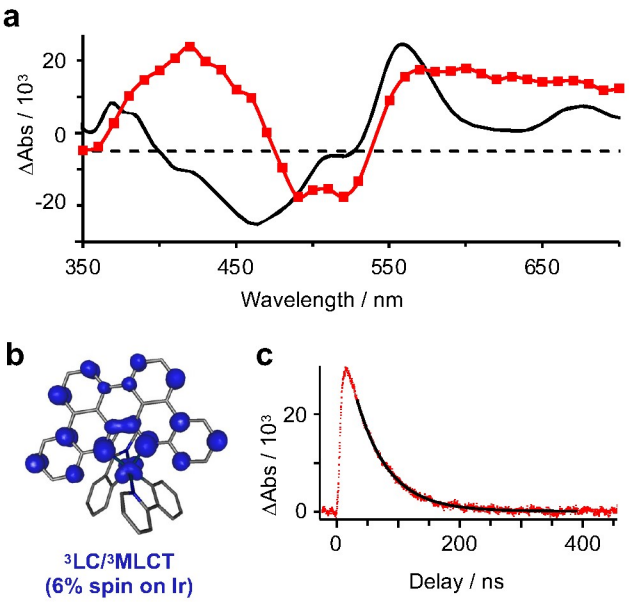

Figure 3. (a) Full spectrum optical transient absorption spectroscopy of [**Ir**]PF_6 in acetonitrile (λ_{pump} = 540 nm) at a 13 ns delay in red overlaid with the spectroelectrochemically simulation of the MLCT state in black. (b) Spin-density map of optimized triplet state of [**Ir**]$^+$. (c) Kinetic trace from oTA experiments monitored at 600 nm.

First, we attempted the aerobic hydroxylation of 4-methoxyphenylboronic acid (**Figure 4a**).[17] Irradiation of [**Ir**]$^+$ in the presence of *N,N*-diisopropylethylamine (DIPEA; E_{ox}(DIPEA/DIPEA$^+$) = +0.28 V vs $FcH^{0/+}$)[18,19] leads to photooxidation of DIPEA and reduction of [**Ir**]$^+$ (E_{red}^* = +0.61 V). Electron-transfer from photoreduced [**Ir**] to O_2 in oxygenated CD_3CN then facilitates boronic acid hydroxylation via the superoxide radical.[17] ^{1}H NMR spectroscopy shows 85±11% conversion to the phenol in 20 h using 2 mol% [**Ir**]$^+$ and 740 nm illumination (**Figures S6-S7** and **Table S2**). No conversion occurs without light, and only minor conversion is evident in the absence of [**Ir**]$^+$ (**Figures S8-S9**, **Table S2**). Energy transfer mediated by $^1O_2$ generation and reaction with furfural in alcoholic solution (**Figure 4b**) is similarly effective. Using 1 mol% [**Ir**]$^+$ excited at 740 nm in oxygenated CD_3OD leads to 85±9% conversion to 5-methoxyfuran-2-one over 23 h.[20] When additional oxygen is bubbled in, the reaction progresses further, reaching 92±4% conversion after another 3 h (**Figures S10-S11**, **Table S3**). A volatile side product (formic acid[21]) is evident in the ^{1}H NMR spectrum and can be removed under reduced pressure (**Figure S12**; see **Figure S45** for mechanism). Control reactions again confirmed the necessity of both [**Ir**]$^+$ and light (**Figures S13, S14; Table S3**). These examples are the lowest energy photocatalysis using an Ir(III) photocatalyst reported to date.

We next turned our attention to the thermodynamically challenging hydrodehalogenation of phenacyl halides using 9,10-dihydro-10-methylacridine as a hydride source (DHA; E_{ox} = +0.4 V vs $FcH^{0/+}$).[19,22] DHA oxidation can been performed using

View Article Online
DOI: 10.1039/D6SC01462C

$[Ru(bpy)_3]^{2+}$ (bpy = 2,2'-bipyridine) and 450 nm light.[22,23] Here, we find photoexcited $[\mathbf{Ir}]^+$ can smoothly oxidize the even more difficult to oxidize *N*-phenyl analogue 10-methyl-9-phenyl-9,10-dihydroacridine (MPA; E_{ox} = +0.5 V vs $FcH^{0/+}$)[19,24] using 740 nm red light, reducing phenacyl bromide to regenerate the starting catalyst (**Figure 4c**). Given the debate in literature as to the reduction potential of phenacyl bromide,[25,26] we measure it at E_{red} = -1.60 V vs $FcH^{0/+}$ (**Figure S15**). In the presence of excess (3 equivalents) of phenacyl bromide, MPA is completely, and cleanly consumed with only acetophenone and the acridinium bromide salt observed by ^{1}H NMR within 30 min at a loading of 2 mol % $[\mathbf{Ir}]^+$ (**Figures S16-S18**). Reducing the catalyst loading to 0.1 mol %, the reaction still cleanly goes to completion after 65 min (**Figures S19-S22**; 1.6 % min^{-1}). With 2 mol % $[\mathbf{Ir}]^+$, the reaction progresses at a rate of 12.1 % min^{-1} and is complete after 10 min of illumination (**Figure S23, S24**). Control reactions again confirm the critical role of both $[\mathbf{Ir}]^+$ and light (**Figures S25-26**). $[\mathbf{Ir}]^+$ proved quite durable and adding additional equivalents of MPA after the initial batch is consumed restarts catalysis with no loss in activity or selectivity (**Figure S27**).

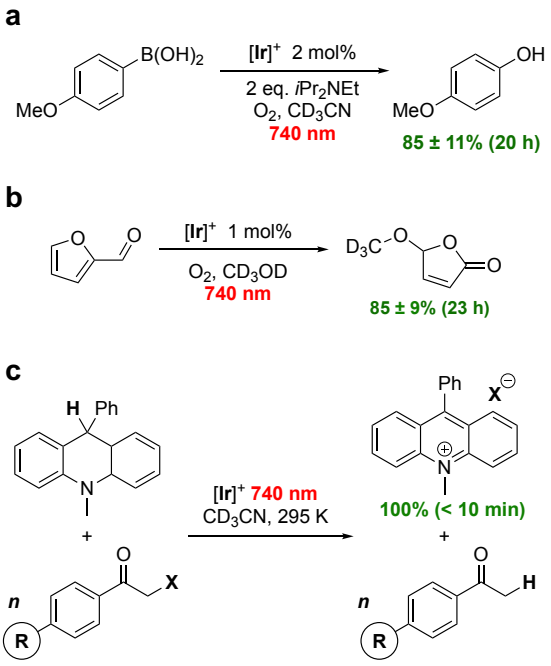

Figure 4. Proof-of-principle photocatalytic reactions using $[\mathbf{Ir}]^+$ and red light (740 nm) illumination.

Using conditions of 2 mol % $[\mathbf{Ir}]^+$ at ambient temperature (295 K), we screened the compatibility of different functional groups using a variety of 4'-functionalized 2-bromoacetophenones (R = H, OMe, Me, F, Cl, CN). In each case, 100% conversion of MPA to the acridinium bromide is observed in the presence of excess (3 equivalents) phenacyl bromide. ^{1}H NMR monitoring (**Figures S28-S33**) allowed us to extract the initial rates (**Figure S34**) which increase with more electron-withdrawing substituents. Comparing the rate versus Hammett parameters (σ_p)[27], however, yielded a poor correlation (**Figure S35**). A better correlation is evident using the substrate reduction potential (**Figure 5**) measured via electrochemistry (**Figures S36-S40**). The influence of the substrate reduction potential is noticeable up to a point: 2-bromo-4'-fluoro- (E_{red} = -1.47 V vs $FcH^{0/+}$) and 2-bromo-4'-cyanoacetophenone (E_{red} = -1.24 V vs $FcH^{0/+}$) are converted at similar rates (**Figure S41**). We postulate that at a certain limit the reaction becomes controlled by diffusion, rather than thermodynamics (grey highlight in **Figure 5**). Exchanging acylbromide for acylchloride in the form of 2-chloroacetophenone (E_{red} = -1.73 V vs $FcH^{0/+}$, **Figure S42**), consumption of MPA is still observed, consistent with MPA photooxidation instigating catalysis, but without clean conversion to the hydrodehalogenated product (**Figure S43**), in line with the thermodynamic challenge presented by this harder-to-reduce substrate.

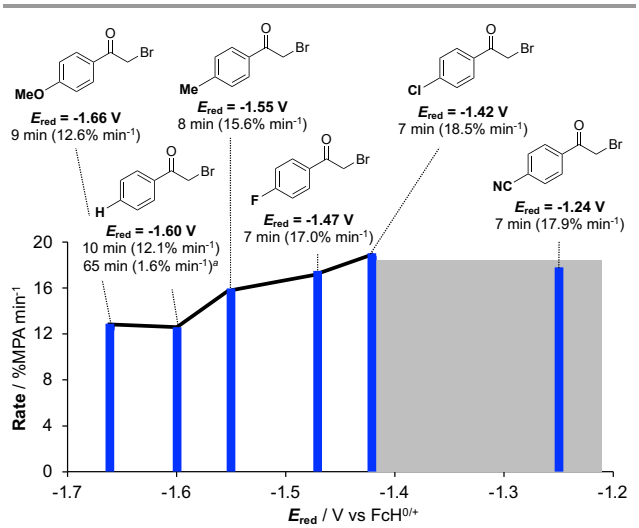

Figure 5. Photocatalytic hydrodehalogenation of 4-substituted phenacyl halides (2 mol% $[\mathbf{Ir}]^+$, 740 nm irradiation; [a] 0.1 mol% $[\mathbf{Ir}]^+$). Potentials are reported versus $FcH^{0/+}$ along with time-to-100% consumption of MPA and the rate of consumption in parentheses (measured by ^{1}H NMR). A black line to guide the eye is overlaid on the data and the diffusion-controlled potential regime beyond which the rate stabilizes is shown in grey.

Conclusions

In summary, we report an Ir(III) complex of the planar, benzannulated π-extended ligand 6,6',7,7'-biphenanthridine ($[\mathbf{Ir}]^+$)[11] can effectively mediate photocatalysis using 740 nm deep red light, the lowest energy illumination reported to date. This represents a 150 nm (3400 cm^{-1}) bathochromic shift from the prior state-of-the-art in low-energy Ir(III) photocatalysis[9,10] and showcases the ability of iridium photocatalysts to reach the deep red/near-infrared region of the electromagnetic spectrum. Direct excitation of $[\mathbf{Ir}]^+$ into its triplet T_n manifold provokes population of a long-lived (55 ns) excited state with strong photoredox properties. The promise of $[\mathbf{Ir}]^+$-mediated deep red photocatalysis is demonstrated through three proof-of-principle reactions, including the aerobic hydroxylation of 4-methoxyphenylboronic acid and $^1O_2$-mediated synthesis of 5-methoxyfuran-2-one. These reactions had not yet been reported possible via red-light iridium photocatalysis.[20] In

View Article Online
DOI: 10.1039/D6SC01462C

addition, we also show $[Ir]^+$ to be capable of hydrodehalogenation via the photooxidation of MPA, a reaction that to the best of our knowledge has been previously only accessible using blue light and the easier to oxidize DHA.[23] Efforts to expand these findings to an greater reaction class scope are currently underway.

Author contributions

Conceptualization: R.J.O., D.E.H. Formal analysis: R.J.O., D.E.H. Funding acquisition: D.E.H. Investigation: R.J.O., D.B.N., M.B., K.A.V. Supervision: D.E.H. Visualization: R.J.O., D.E.H. Writing – original draft: R.J.O., D.E.H. Writing – review & editing: R.J.O., D.E.H.

Conflicts of interest

There are no conflicts to declare.

Acknowledgements

Support for this work came from the Natural Sciences Engineering Research Council of Canada (RGPIN-2022-04501; CGS-D / Michael Smith Foreign Study Supplement) and Compute Canada. We are grateful to Prof. James K. McCusker for access to TA instrumentation, training, and insightful discussions, as well as to Bekah Bowers for assistance with TA measurements.

Data availability

The data supporting this article have been included as part of the Supplementary Information. Supplementary information: supporting computational data, NMR spectra, electrochemical plots, time-resolved spectroscopy data, and further experimental details. See DOI: [URL – format https://doi.org/DOI]

References

1 E. G. Moschetta, G. C. Cook, L. J. Edwards, M. A. Ischay, Z. Lei, F. Buono, F. Lévesque, J. A. O. Garber, M. MacTaggart, M. Sezen-Edmonds, K. P. Cole, M. G. Beaver, J. Doerfler, S. M. Opalka, W. Liang, P. D. Morse and N. Miyake, *Org. Process Res. Dev.*, 2024, **28**, 831–846.
2 N. A. Romero and D. A. Nicewicz, *Chem. Rev.*, 2016, **116**, 10075–10166.
3 D. C. Cabanero and T. Rovis, *Nat. Rev. Chem.*, 2025, **9**, 28–45.
4 N. Kumar, T. Sharma, N. Thakur, R. Jain and N. Sinha, *Chem. - Eur. J.*, 2025, **31**, e202500365.
5 L. Fortier, C. Lefebvre and N. Hoffmann, *Beilstein J. Org. Chem.*, 2025, **21**, 296–326.
6 M. Zhong and Y. Sun, *Chem. Catal.*, 2024, **4**, 100973.
7 G. Chacktas, B. Pfund, T. Kerackian, P. Yaltseva, M. Villeneuve, D. Durand, N. Fabre, C. Fiorini-Debuisschert, J.-C. Cintrat, O. S. Wenger and E. Romero, *ACS Catal.*, 2025, **15**, 13938–13947.
8 K. Teegardin, J. I. Day, J. Chan and J. Weaver, *Org. Process Res. Dev.*, 2016, **20**, 1156–1163.
9 K. A. Xie, E. Bednarova, C. L. Joe, C. Lin, T. C. Sherwood, E. M. Simmons, B. C. Lainhart and T. Rovis, *J. Am. Chem. Soc.*, 2023, **145**, 19925–19931.
10 E. Bednářová, R. Grotjahn, C. Lin, K. A. Xie, Y. Karube, J. S. Owen, C. L. Joe, B. C. Lainhart, T. C. Sherwood and T. Rovis, *J. Am. Chem. Soc.*, 2025, **147**, 12511–12522.
11 D. B. Nemez, R. J. Ortiz, K. A. Veilleux, J. A. G. Williams and D. E. Herbert, *Chem.-Eur. J.*, 2025, **31**, e01802.
12 D. B. Nemez, I. B. Lozada, J. D. Braun, J. A. G. Williams and D. E. Herbert, *Inorg. Chem.*, 2022, **61**, 13386–13398.
13 J. T. Yarranton and J. K. McCusker, *J. Am. Chem. Soc.*, 2022, **144**, 12488–12500.
14 L. Schmid, F. Glaser, R. Schaer and O. S. Wenger, *J. Am. Chem. Soc.*, 2022, **144**, 963–976.
15 M. V. Wee-Léonard, B. Elias and L. Troian-Gautier, *J. Am. Chem. Soc.*, 2024, **146**, 11031–11035.
16 D. Kim and T. S. Teets, *Chem. Phys. Rev.*, 2022, **3**, 021302.
17 Y.-Q. Zou, J.-R. Chen, X.-P. Liu, L.-Q. Lu, R. L. Davis, K. A. Jørgensen and W.-J. Xiao, *Angew. Chem., Int. Ed.*, 2012, **51**, 784–788.
18 Y. Kwon, J. Lee, Y. Noh, D. Kim, Y. Lee, C. Yu, J. C. Roldao, S. Feng, J. Gierschner, R. Wannemacher and M. S. Kwon, *Nat. Commun.*, 2023, **14**, 92.
19 N. G. Connelly and W. E. Geiger, *Chem. Rev.*, 1996, **96**, 877–910.
20 B. D. Ravetz, N. E. S. Tay, C. L. Joe, M. Sezen-Edmonds, M. A. Schmidt, Y. Tan, J. M. Janey, M. D. Eastgate and T. Rovis, *ACS Cent. Sci.*, 2020, **6**, 2053–2059.
21 B. L. Feringa, *Recl. Trav. Chim. Pays-Bas*, 1987, **106**, 469–488.
22 S. Fukuzumi, S. Mochizuki and T. Tanaka, *J. Phys. Chem.*, 1990, **94**, 722–726.
23 C. K. Prier, D. A. Rankic and D. W. C. MacMillan, *Chem. Rev.*, 2013, **113**, 5322–5363.
24 N. W. Koper, S. A. Jonker, J. W. Verhoeven and C. van Dijk, *Recl. Trav. Chim. Pays-Bas*, 1985, **104**, 296–302.
25 D. D. Tanner and H. K. Singh, *J. Org. Chem.*, 1986, **51**, 5182–5186.
26 E. Speckmeier, P. J. W. Fuchs and K. Zeitler, *Chem. Sci.*, 2018, **9**, 7096–7103.
27 C. Hansch, A. Leo and R. W. Taft, *Chem. Rev.*, 1991, **91**, 165–195.

View Article Online
DOI: 10.1039/D6SC01462C

The data supporting this article have been included as part of the Supplementary Information. Supplementary information: supporting computational data, NMR spectra, electrochemical plots, time-resolved spectroscopy data, and further experimental details. See DOI: [URL – format https://doi.org/DOI]